

Articles

Reactions of Sn(NMe₂)₂ with Primary Aryl Phosphides, ArPH⁻: Synthesis and Structures of the Heteroleptic Cages [(PhP–PPh)Sn(μ–PPh)]₂(Na·PMDETA)₄ and [{Sn(μ₃-Ppy)]₃{Sn(μ₃,μ₁-pyP–Ppy)]₃

Felipe García,[†] Alexander D. Hopkins,[†] Richard A. Kowenicki,[†] Mary McPartlin,[‡] Christopher M. Pask,[†] Matthew L. Stead,[†] Anthony D. Woods,^{*,†} and Dominic S. Wright^{*,†}

Chemistry Department, University of Cambridge, Lensfield Road, Cambridge CB2 1EW, U.K., and Department of Health and Biological Sciences, London Metropolitan University, London N7 8DB, U.K.

Received October 22, 2004

The reaction of Sn(NMe₂)₂ with the primary phosphido alkali metal complex PhPHNa (1:2 equiv, respectively) in the presence of the Lewis base donor PMDETA [(Me₂NCH₂CH₂)₂-NMe] gives the heterometallic cage [(PhP–PPh)Sn(μ–PPh)]₂(Na·PMDETA)₄ (**1**), containing the novel [(PhP–PPh)Sn(μ–PPh)]₂⁴⁻ tetraanion. The analogous reaction using pyPHLi (py = 2-pyridyl) in THF/toluene as the solvent gives the neutral cage [{Sn(μ₃-Ppy)]₃{Sn(μ₃,μ₁-pyP–Ppy)]₃ (**2**), having a unique “stacked” propeller arrangement in the solid state.

Introduction

In contrast to their imido counterparts, which function as robust ligands to a range of metals,¹ heterometallic group 15/alkali metal phosphinidene cages such as [{Sb(PR)₃}]₂Li₆·6L (R = Cy, ^tBu; L = Me₂NH, THF) are thermally unstable and can be isolated only at low temperature (ca. 0–25 °C).² At higher temperatures (ca. 30–100 °C) such cages decompose via heterocyclic intermediates of the type [(RP)_nE]⁻ (n = 3 or 4) to form Zintl compounds containing E_n^{x-} anions. Underlying the difference in behavior between nitrogen and phosphorus cages of this type is the stability of the P–P bond, which has the greatest homoatomic single-bond energy between any of the group 15 elements.³ This factor provides a potentially general thermodynamic driving force for the formation of a very broad range of new metal–metal and P–P bonded molecular species elsewhere in the periodic table. Our recent studies have shown that analogous heterometallic Sn(II) phosphinidene cages exhibit the same overall reactivity trends as those found for group 15.⁴ In particular reactions of aliphatic lithium phosphides [RPHLi] (R = Cy, ^tBu) with the Sn(II) base Sn(NMe₂)₂ in THF result in the formation of the metallacyclic [{Sn(μ–PR)]₂(μ–PR)]₂⁴⁻ tetraan-

ion, whereas the heteroleptic [{Sn(μ–PMes)]₂(MesP–PMes)]₂²⁻ (Mes = 2,4,6-Me₃C₆H₂) dianion, containing a P–P coupled [MesP–PMes]²⁻ ligand, is produced by the analogous reaction involving the aryl phosphide MesPHLi in the presence of TMEDA (Me₂NCH₂CH₂NMe₂).^{4a} The formation of the [{Sn(μ–PR)]₂(μ–PR)]₂⁴⁻ and [{Sn(μ–PMes)]₂(MesP–PMes)]₂²⁻ anions in these closely related reactions can be understood in terms of the mechanism shown in Scheme 1, in which the key intermediate **A** can eliminate either H₂ (to give the dianion) or RPH₂ (to give the tetraanion).⁵

Further support for this mechanism was provided by a recent study that showed that the [Sn₂(μ–PMes)]₃²⁻ dianion (the monomer unit of the metallacyclic [{Sn(μ–PR)]₂(μ–PR)]₂⁴⁻ tetraanion) is obtained by the reaction of Sn(NMe₂)₂ with MesPHK in the absence of TMEDA (rather than the P–P coupled [{Sn(μ–PMes)]₂(MesP–PMes)]₂²⁻ dianion).⁶ This result presumably reflects the lower nucleophilicity of the MesPH⁻ anion in the absence of strong Lewis base chelation of the alkali metal cation (Scheme 2) and shows the potentially important influence of the donor on the outcomes of these reactions.

* To whom correspondence should be addressed. E-mail: dsw1000@cus.cam.ac.uk. Fax: 01223 336362.

[†] University of Cambridge.

[‡] London Metropolitan University.

(1) Beswick, M. A.; Wright, D. S., *Coord. Chem. Rev.* **1998**, *176*, 373.

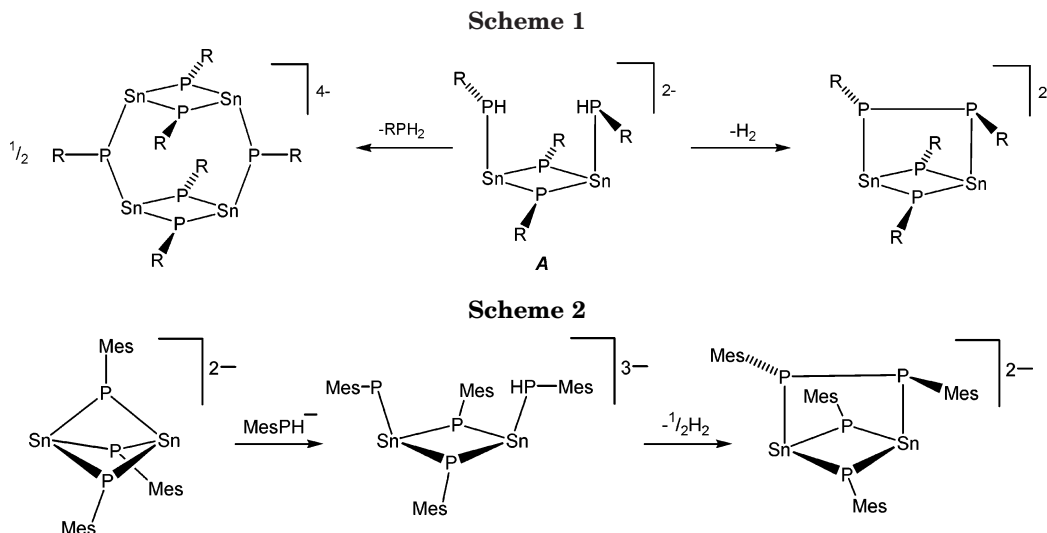
(2) (a) Hopkins, A. D.; Wood, J. A.; Wright, D. S.; Hopkins, A. D.; Wood, J. A.; Wright, D. S. *Coord. Chem. Rev.* **2001**, *216*, 155. (b) Beswick, M. A.; Choi, N.; Harmer, C. N.; Hopkins, A. D.; McPartlin, M.; Wright, D. S. *Science* **1998**, *281*, 1500.

(3) *Inorganic Chemistry; Principles of Structure and Reactivity*, 4th ed.; Huheey, J. E., Keiter, E. A., Keiter, R. L., Eds.; 1993; p A21.

(4) (a) Davies, J. E.; Hopkins, A. D.; Rothenberger, A.; Woods, A. D.; Wright, D. S. *J. Chem. Soc., Chem. Commun.* **2001**, 525. (b) Alvarez-Bercedo, P.; Bond, A. D.; Haigh, R.; Hopkins, A. D.; Lawson, G. T.; McPartlin, M.; Moncrieff, D.; Gonzalez Mosquera, M. E.; Rawson, J. M.; Woods, A. D.; Wright, D. S. *J. Chem. Soc., Chem. Commun.* **2003**, 1288. (c) Alvarez-Bercedo, P.; Lawson, G. T.; Mosquera, M. E. G.; McPartlin, M.; Moncrieff, D.; Woods, A. D.; Wright, D. S., unpublished results.

(5) García, F.; Hopkins, A. D.; Pask, C. M.; Woods, A. D.; Wright, D. S. *J. Mater. Chem.* **2004**, *21*, 3091.

(6) García, F.; Hopkins, A. D.; Humphrey, S. M.; McPartlin, M.; Pask, C. M.; Woods, A. D.; Wright, D. S. *Organometallics*, in press.



We report here studies of the reactions of alkali metal primary aryl phosphides RPH^- with $\text{Sn}(\text{NMe}_2)_2$. The syntheses and structures of the new complexes $[\{(\text{PhP}-\text{PPh})\text{Sn}(\mu\text{-PPh})_2(\text{Na}\cdot\text{PMDETA})_4\}]$ (**1**) [$\text{PMDETA} = \{\text{Me}_2\text{-NCH}_2\text{CH}_2\}_2\text{NMe}$] and $[\{\text{Sn}(\mu_3\text{-Ppy})_3\{\text{Sn}(\mu_3,\mu_1\text{-pyP-Ppy})\}_3\}]$ (**2**) ($\text{py} = 2\text{-pyridyl}$) are reported, **1** containing the novel $[(\text{PhP}-\text{PPh})\text{Sn}(\mu\text{-PPh})_2]^{4-}$ tetraanion and **2** containing the first example of a donor-functionalized oligophosphide ligand in any metal complex. These new arrangements represent key structural types in the series of heteroleptic $\text{Sn}(\text{II})$ complexes containing $[\text{RP}-\text{PR}]^{2-}/\text{RP}^{2-}$ ligands.

Results and Discussion

The new compounds **1** and **2** were prepared in similar ways, by the 1:2 stoichiometric reactions of $\text{Sn}(\text{NMe}_2)_2$ with PhPHNa or pyPHLi in THF. **1** was then crystallized from PMDETA in toluene, whereas **2** was crystallized from THF/toluene. The extreme air- and moisture-sensitivity of both complexes made their characterization by spectroscopic and analytical means particularly difficult. Later structural characterization of **1** shows that it is crystallized initially as the toluene solvate **1**·toluene. However, placing this solvate under vacuum during isolation (ca. 15 min, 10^{-1} atm) leads to complete desolvation, as shown by ^1H NMR spectroscopy and elemental analysis. The low solubility of **1** once isolated (even in THF) made definitive ^{31}P NMR studies impossible, the spectrum consisting of a mixture of species in the region $\delta -124$ to -128 [including some unavoidable hydrolysis into PhPH_2 ($\delta -125.3$)]. As a result of the low solubility of **1**, the ^1H NMR spectrum is consistent largely with the presence of uncoordinated PMDETA ($\delta 2.35\text{--}2.13$), with the phenyl resonances ($\delta 8.7\text{--}6.6$) being of only very low relative abundance with respect to PMDETA. For this reason, meaningful integration of the spectrum could not be accomplished. Although later structural characterization shows that **2** is crystallized as the THF solvate **2**·2.5THF initially, elemental analysis of samples of **2** that have been dried under vacuum (ca. 20 min, 10^{-1} atm) suggests that only about one of the lattice-bound THF ligands remains. Like **1**, the ^{31}P NMR spectrum of the complex is complicated and little definitive information could be obtained concerning the nature of the solution species present,

Table 1. Structure Solution and Refinements of the Solvates **1·Toluene and **2**·2.5THF^a**

	1 ·toluene	2 ·2.5THF
empirical formula	$\text{C}_{79}\text{H}_{130}\text{N}_{12}\text{Na}_4\text{P}_6\text{Sn}_2$	$\text{C}_{55}\text{H}_{56}\text{N}_9\text{O}_{2.5}\text{P}_9\text{Sn}_6$
fw	1763.11	1873.96
cryst syst	monoclinic	triclinic
space group	$C2/c$	$P1$
a (Å)	22.058(4)	11.810(2)
b (Å)	18.543(4)	14.816(3)
c (Å)	25.931(5)	19.365(4)
α (deg)		90.93(3)
β (deg)	109.20(3)	92.14(3)
γ (deg)		101.67(3)
Z	4	2
V (Å ³)	10017(3)	3315.0(12)
ρ (calc) (Mg m^{-3})	1.169	1.877
μ (Mo $K\alpha$) (mm^{-1})	0.654	2.490
$F(000)$	3688	1808
no. of reflns collected	15 507	37 212
cryst size (mm)	$0.23 \times 0.18 \times 0.16$	$0.23 \times 0.05 \times 0.05$
θ range (deg)	3.61–22.00	3.52–27.51
no. of indep reflns (R_{int})	5953(0.051)	15096(0.046)
absorb corr	semiempirical from equivalents	semiempirical from equivalents
max., min. transmn	0.676, 0.631	0.886, 0.598
no. of data/restraints/params	5953/5/460	15 096/48/726
goodness-of-fit on F^2	1.144	1.087
R indices [$I > 2\sigma(I)$]	$R1 = 0.063,$ $wR2 = 0.151$	$R1 = 0.047,$ $wR2 = 0.080$
R indices (all data)	$R1 = 0.084,$ $wR2 = 0.159$	$R1 = 0.077,$ $wR2 = 0.091$
largest peak and hole ($e \text{ \AA}^{-3}$)	0.871, -0.328	0.800, -0.749

^a Data in common; $T = 180(2)$ K, $\lambda = 0.71073$ Å.

the spectrum consisting of groups of overlapping multiplets in the region $\delta -60$ to -75 . Despite repeated attempts, no ^{119}Sn resonances could be detected for **1** and **2**.

Low-temperature (192 K) X-ray crystallographic studies of the solvates **1**·toluene and **2**·2.5THF were undertaken. Details of the structure solutions and data refinements are given in Table 1, while selected bond lengths for **1**·toluene and **2**·2.5THF are provided in Tables 2 and 3, respectively.

The low-temperature X-ray analysis of **1** shows that the complex consists of centrosymmetric cage molecules $[\{(\text{PhP}-\text{PPh})\text{Sn}(\mu\text{-PPh})_2(\text{Na}\cdot\text{PMDETA})_4\}]$ (Figure 1a), which result from the association of the $[\{(\text{PhP}-\text{PPh})\text{Sn}(\mu\text{-PPh})_2\}]^{4-}$ tetraanion with four PMDETA-solvated Na^+ cations. In addition, there is one toluene molecule in the lattice per molecule of **1**. The heteroleptic $[\{(\text{PhP}-$

Table 2. Selected Bond Lengths and Angles for the Solvate 1·0.5Toluene

Bond Lengths (Å) ^a			
Sn(1)–P(1)	2.631(2)	Na(1)–P(2A)	2.983(4)
Sn(1)–P(2)	2.604(2)	Na(1)–P(3)	3.031(4)
Sn(1)–P(2A)	2.599(2)	Na(2)–P(3)	2.888(4)
Sn(1)–Na(2)	3.267(3)	P(1)–P(3)	2.185(3)
Na(1)–P(1)	3.371(4)	Na(1,2)–N(PMDETA)	2.49(1)–2.583(8)
Bond Angles (deg)			
P(2)–Sn(1)–P(2A)	86.11(7)	P(3)–Na(1)–P(1)	39.47(6)
P(2)–Sn(1)–P(1)	102.21(7)	P(1)–Na(1)–P(2A)	75.70(8)
P(2A)–Sn(1)–P(1)	96.79(7)	P(3)–Na(1)–P(2A)	94.2(1)
Sn(1)–P(1)–P(3)	87.03(9)	P(3)–Na(2)–Sn(1)	65.21(7)
Sn(1)–P(2)–Sn(1A)	83.89(6)		

^a Symmetry transformations used to generate equivalent atoms A $-x, y, -z+1/2$.

$\text{PPh})\text{Sn}(\mu\text{-PPh})_2]^{4-}$ tetraanion is composed of a central Sn_2P_2 ring unit with terminal PhP-PPh diphosphide groups bonded to each Sn(II) center. The most closely related Sn(II) framework of this type is the homoleptic $[\text{Me}_3\text{SiPSn}(\mu\text{-PSiMe}_3)_2]^{4-}$ tetraanion, again being composed of a Sn_2P_2 ring unit but with terminal PSiMe_3 groups attached to each of the Sn(II) centers.^{7,8}

The Sn–P [range 2.599(2)–2.631(2)Å] and P–P [P(1)–P(3) 2.185(3) Å] bonds within the Sn_2P_6 fragment of the $\{[(\text{PhP-PPh})\text{Sn}(\mu\text{-PPh})_2]^{4-}$ tetraanion of **1** are within the range of values reported previously for Sn(II)–P^{4,8,9} and P–P¹⁰ single bonds. The Sn_2P_2 ring of the tetraanion is highly puckered [by an angle of 47.7° about the P(2)⋯P(2A) vector], with the terminal PhP-PPh groups adopting a *cis* conformation. All of the Sn and P centers are involved in bonding to the four Na⁺ counterions. The coordination of Na(1) is particularly unusual, involving side-on (η^2 -type) bonding of both of the P centers of a terminal PhP-PPh group [P(1)–Na(1) 3.371(4) Å, P(3)–Na(1) 3.031(4) Å] as well as bonding to the μ_2 - PhP group of the Sn_2P_2 ring unit of the tetraanion [Na(1)–P(2A) 2.983(4) Å]. Na(2) is coordinated by the terminal P center of a PhP-PPh group [P(3)–Na(2) 2.888(4) Å] as well as by the lone pair of one of the Sn(II) centers [Sn(1)–Na(2) 3.267(3) Å]. Although only a few examples of Sn–Na bonds have been structurally authenticated, the bonds in **1** are within the range of values observed previously [range 3.07–3.39 Å].^{4b,11} The further coordination of tridentate PMDETA ligands to Na(2) and Na(1) results in highly distorted five- and six-coordinate geometries, respectively, for these ions.

The low-temperature X-ray structure of **2** shows that the compound has a pseudo- C_3 symmetric, hexanuclear

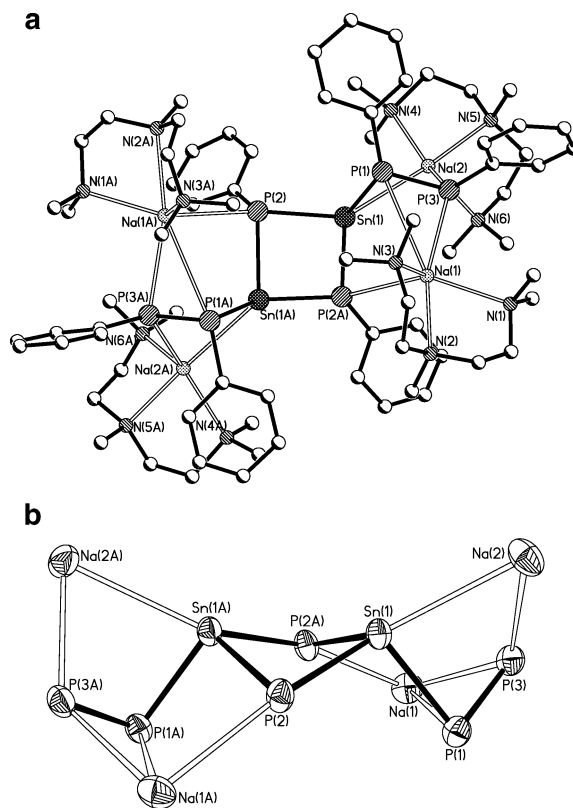


Figure 1. (a) Ball-and-stick plot of molecules of **1** (H atoms and the lattice toluene molecules have been omitted for clarity). (b) Thermal ellipsoid plot of the core, drawn at the 40% probability level.

“stack” arrangement in the solid state (Figure 2a), which can be regarded as resulting from the association of a $[\text{Sn}(\mu\text{-Ppy})_3]$ phosphinidine ring unit [involving Sn(4), Sn(5), and Sn(6)] with a diphosphide $[\text{Sn}(\mu\text{-pyP-Ppy})_3]$ ring unit [involving Sn(1), Sn(2), and Sn(3)]. In addition, there are a total of two and a half THF molecules in the lattice. The overall architecture of the Sn_6P_9 core of **2** is that of a “propeller” arrangement in which the three pyP-Ppy ligands form the blades (Figure 2b). Only a few Sn(II) phosphinidine compounds^{4,8,9} and only one Sn(II) oligophosphide compound^{4a} have been reported in the literature, the most closely related species to **2** being the neutral, homoleptic Sn_6 stack $[\text{Sn}(\mu_3\text{-PSi}^i\text{-Pr}_3)]_6$.^{9b} To our knowledge, the arrangement of the core of **2** and the presence of donor-functionalized diphosphide ligands in this compound are unique features.

Table 3. Selected Bond Lengths and Angles for the Solvate 2·2.5THF

Bond Lengths (Å)			
Sn(1)–P(1)	2.594(2)	Sn(3)–N(92)	2.497(5)
Sn(1)–P(3)	2.852(2)	Sn(4)–P(4)	2.670(2)
Sn(1)–P(5)	2.625(2)	Sn(4)–P(5)	2.598(2)
Sn(1)–N(72)	2.431(6)	Sn(4)–P(7)	2.662(2)
Sn(2)–P(1)	2.860(2)	Sn(5)–P(6)	2.630(2)
Sn(2)–P(2)	2.585(2)	Sn(5)–P(5)	2.639(2)
Sn(2)–P(4)	2.602(2)	Sn(5)–P(9)	2.630(2)
Sn(2)–N(82)	2.498(5)	Sn(6)–P(4)	2.624(2)
Sn(3)–P(2)	2.884(2)	Sn(6)–P(6)	2.648(2)
Sn(3)–P(3)	2.578(2)	Sn(6)–P(8)	2.656(2)
Sn(3)–P(6)	2.616(2)	P–P range	2.183(2)–2.184(2)
Bond Angles (deg)			
P–Sn(1,2,3)–P range	81.46(6)–93.68(6)	Sn–P(4,5,6)–Sn range	112.99(6)–124.12(7)
P–Sn(4,5,6)–P range	87.71(6)–94.67(6)	N–Sn(1,2,3)–P(3,1,2) range	163.4(1)–164.7(1)
Sn–P(1,2,3)–Sn range	144.98(7)–145.62(7)	P–P–Sn(4,5,6) range	96.67(7)–98.60(7)

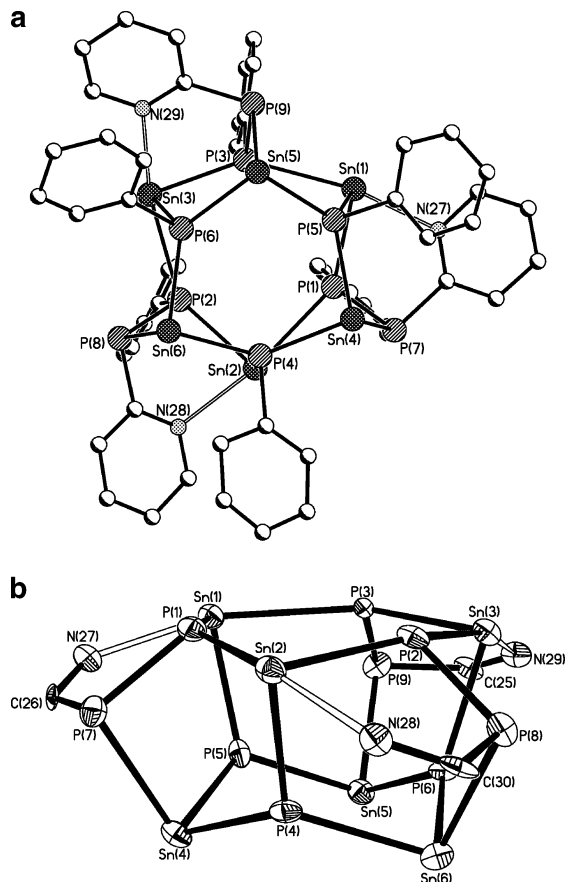


Figure 2. (a) Ball-and-stick plot of **2** (H atoms and lattice THF molecules have been removed for clarity). (b) Thermal ellipsoid plot of molecules of the side-view of the core, drawn at the 40% probability level.

The association of the phosphinidene and diphosphide ring units of **1** results from a combination of μ_3 -bridging of the Ppy groups and μ_1, μ_2 -bridging of the pyP–Ppy ligands between the trimeric ring constituents. In addition to the Sn–P bonding within the core, one of the py groups of each of the pyPPpy ligands forms Sn...N donor interactions with the Sn centers within the $[\text{Sn}(\mu\text{-pyPPpy})_3]$ ring unit [Sn(1,2,3)...N(72,82,92) range 2.431(6)–2.497(5) Å].¹¹ Consequently, the Sn centers within the $[\text{Sn}(\mu\text{-Ppy})_3]$ ring have pseudo-tetrahedral geometries [P–Sn(4,5,6)–P range 87.71(6)–94.66(6)°], while those within the $[\text{Sn}(\mu\text{-pyP–Ppy})_3]$ ring have pseudo-trigonal bipyramidal geometries [P–Sn–

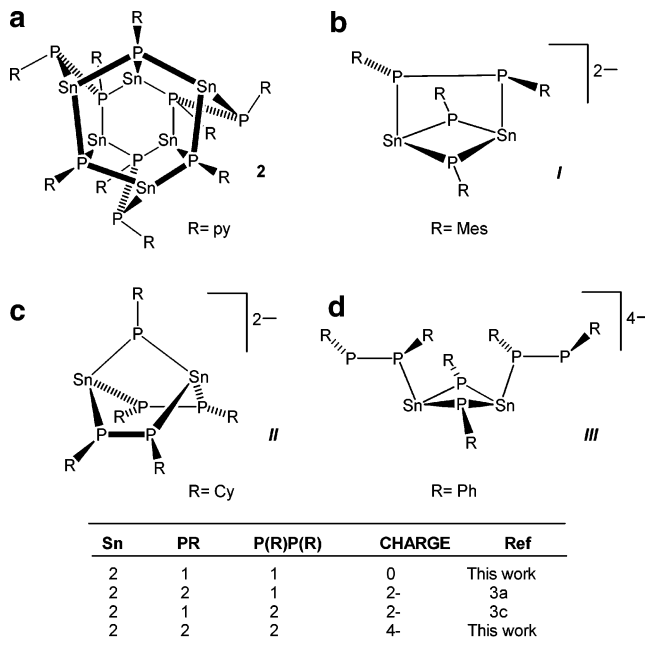


Figure 3. Core structures of (a) **2**, (b) **I**, (c) **II**, and (d) **III**.

(1,2,3)–P range 81.46(6)–93.68(6)°]. The remaining coordination position in each set of Sn coordination environment is occupied by a stereochemically active Sn lone pair. The axial coordination of the pyridyl-N atoms to the trigonal bipyramidal Sn centers introduces a marked distortion in the core structure, resulting in a noticeable elongation of the Sn–P bonds *trans* to the pyridyl-N atoms [Sn(1,2,3)–P(3,1,2) range 2.852(2)–2.884(2) Å] compared to the other Sn–P bonds [range 2.578(2)–2.670(2) Å] [cf. 2.611(3)–2.671(3) Å in the phosphinidene hexamer $[\text{Sn}(\mu_3\text{-PSi}^i\text{Pr}_3)_6]^{6b}$]. In addition, this coordination and the bridging of the pyP–Ppy ligands between the Sn_3P_3 ring units appears to introduce considerable strain into the core structure of **1**, as seen in the unusually large internal Sn–P–Sn angles at the μ_2 -bridging P centers [P(1), P(2), and P(3)] of the pyP–Ppy ligands [range 144.98(7)–145.62(6)°] and in the flattening of the $[\text{Sn}(\mu\text{-pyP–Ppy})_3]$ ring unit [Sn(1)P(1)Sn(2)P(2)Sn(3)P(3) being coplanar to within 0.18 Å] compared to the $[\text{Sn}(\mu\text{-Ppy})_3]$ ring [Sn(4)P(4)Sn(5)P(5)Sn(6)P(6), which is only coplanar to within 0.49 Å] (Figure 2b). The P–P bonds within the pyP–Ppy ligands of **1** (mean 2.183 Å) are typical of single P–P bonds.¹⁰

Closing Remarks

The significance of the observation of the new frameworks of **1** and **2** in the current work is that these species represent previously unobserved stoichiometries that complete the series of simple heteroleptic phosphinidene/diphosphide complexes of this type (as illustrated in Figure 3). It can be noted in this regard that other apparently possible compositions would correspond to large net charges on the anion units that would probably render them inaccessible (e.g., 1:2:2 of $\text{Sn:RP}^{2-}:\text{RP–PR}^{2-}$ would correspond to a hexaanion). Comparison of the Sn(II)-phosphorus frameworks of **1** (**III**, Figure 3d) and **2** (Figure 3a) with the previously characterized heteroleptic phosphinidene/diphosphide dianions $[\{\text{Sn}(\mu\text{-PMes})_2(\text{MesP–PMes})\}_2]^{2,3a}$ (**II**, Figure 3b) and $[\{\text{Sn}(\text{MesP–PMes})_2(\mu\text{-PMes})\}_2]^{2,3c}$ (**II**, Figure 3c)

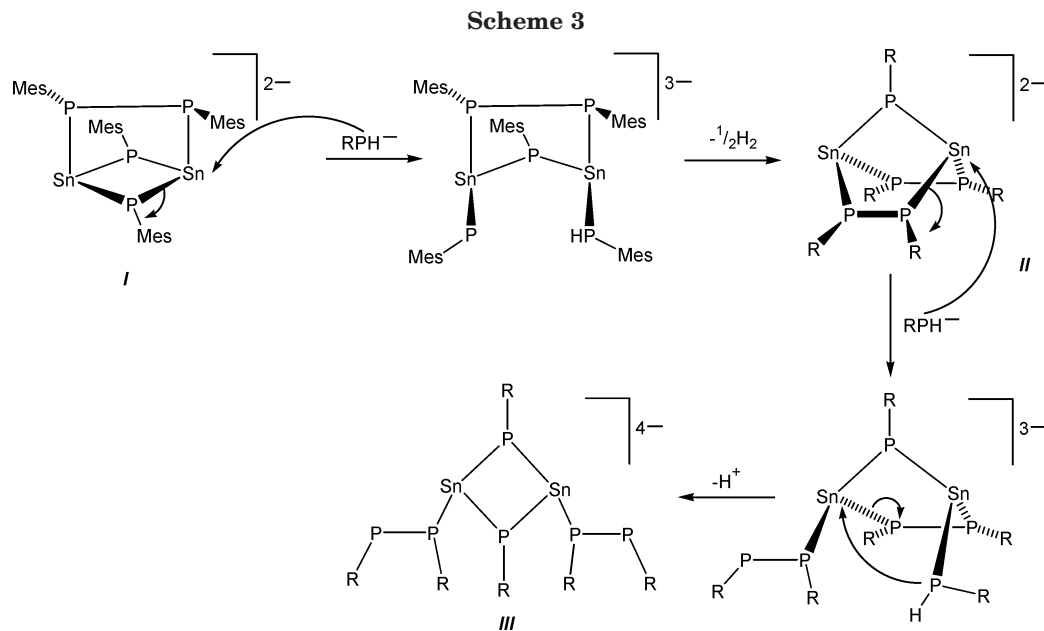
(7) Westerhausen, M.; Schwarz, W. *Z. Anorg. Allg. Chem.* **1996**, *622*, 903.

(8) For further examples of heterometallic alkali and alkaline earth metal/Sn(II) phosphides (in addition to those listed in ref 3), see: Allan, R. E.; Beswick, M. A.; Cromhout, N. L.; Paver, M. A.; Raithby, P. R.; Steiner, A.; Trevithick, M.; Wright, D. S. *J. Chem. Soc., Chem. Commun.* **1501**, 1996. Westerhausen, M.; Low, R.; Schwarz, W. *J. Organomet. Chem.* **1996**, *513*, 213. Westerhausen, M.; Hausen, H.-D.; Schwarz, W. *Z. Anorg. Allg. Chem.* **1995**, *621*, 877.

(9) For neutral compounds of the type $[\text{SnPR}]_n$ see: (a) Westerhausen, M.; Krofta, K.; Wiberg, N.; Nöth, H.; Pfitzer, A. *Z. Naturforsch.* **1998**, *53B*, 1489. (b) Driess, M.; Martin, S.; Merz, K.; Pintchouk, V.; Pritzkow, H.; Grützmacher, H. *Angew. Chem., Int. Ed. Engl.* **1997**, *36*, 1896.

(10) Conquest software for searching the Cambridge Structural Data Base and Visualizing Crystal Structures (January 2004): Bruno, I. J.; Cole, J. C.; Edgington, P. R.; Kessler, M.; Macrae, C. F.; McCabe, P.; Pearson, J.; Taylor, R. *Acta Crystallogr.* **2001**, *B58*, 389.

(11) Klinkhammer, K. W. *Chem. Eur. J.* **1997**, *3*, 1418. Pu, L.; Haubrich, S. T.; Power, P. P. *J. Organomet. Chem.* **1999**, *582*, 100. Wiberg, N.; Wagner, H.-W.; Nöth, H.; Seifert, T. *Z. Naturforsch.* **1999**, *3*, 1418.



shows that these species are related by successive formal addition of RP units. This relationship may have a deeper significance as far as the mechanism involved in the formation of at least some of these species is concerned. We have suggested previously that **II** is derived from **I** by a mechanism involving nucleophilic addition of MesPH^- to $\text{Sn}(\text{II})$, followed by elimination of molecular H_2 (Scheme 3).^{4c} This mechanism is a main group counterpart of that proposed previously by Stephan and co-workers in the formation of the oligophosphides $[\text{Cp}^*\text{Zr}(\text{PR})_3]$ in the thermolysis reactions of $[\text{Cp}^*\text{Zr}(\text{PHR})_2]$.¹³ A similar mechanism involving nucleophilic addition of RPH^- to the framework of **II** followed by deprotonation would explain the formation of **III** (Scheme 3). Overall, our combined studies indicate that the extent of these reactions and the nature of the final products generated are dependent on (i) the electronic and steric nature of the organic group (R), (ii) the alkali metal, and (iii) the presence of Lewis base donor. It is significant in respect to the proposed mechanisms discussed in Scheme 3 that all of these factors will have a direct effect on the nucleophilicity/basicity of the RPH^- anion. The subtle influence of these factors is stressed in the current study by the formation of the very different products **1** and **2** in closely related reactions.

Experimental Section

The reagents $[\text{Sn}(\text{NMe}_2)_2]$, PhCH_2Na , pyPH_2 , and PhPH_2 and the new compounds **1** and **2** are air- and moisture-sensitive. They were handled on a vacuum line using standard inert-atmosphere techniques and under dry/oxygen-free argon. $\text{Sn}(\text{NMe}_2)_2$,¹⁴ pyPH_2 ,¹⁵ and PhCH_2K ¹⁶ were prepared using the

literature methods, and PhPH_2 was acquired commercially (Aldrich). Since $\text{Sn}(\text{NMe}_2)_2$ is thermally unstable, it was stored as a solid at -15°C . Solvents (toluene and THF) were dried over Na/benzophenone prior to reactions. Complexes **1** and **2** were isolated and characterized with the aid of a nitrogen-filled glovebox fitted with a Belle Technology O_2 and H_2O internal recirculation system. Melting points (uncorrected) were determined by using a conventional apparatus and sealing samples in capillaries under nitrogen. IR spectra were recorded as Nujol mulls using NaCl plates and were run on a Perkin-Elmer Paragon 1000 FTIR spectrophotometer. Elemental analyses were performed by first sealing the samples under nitrogen in airtight aluminum boats (1–2 mg), and C, H, N, and P content was analyzed using an Exeter Analytical CE-440. ^1H and ^{31}P NMR spectra were recorded on a Bruker Advance 400 MHz FT spectrometer in dry deuterated $\text{D}_8\text{-THF}$ (using the solvent resonances as the internal reference for ^1H and an external standard of 85% $\text{H}_3\text{PO}_4/\text{D}_2\text{O}$ for ^{31}P).

Synthesis of 1. To a solution of PhCH_2Na (0.57 g, 5.0 mmol) in THF (20 mL) at -78°C was added PhPH_2 (0.5 mL, 5.0 mmol), giving an orange solution. The solution was stirred at room temperature (4 h) before being cooled to -78°C . $\text{Sn}(\text{NMe}_2)_2$ (0.52 g, 2.5 mmol) in THF (10 mL) was added, and the solution turned dark orange immediately. The reaction was allowed to stir at room temperature (16 h). The solvent was removed, and the product was crystallized at -15°C (24 h) from a toluene (ca. 20 mL)/PMDETA (ca. 15 mL) solution. Placing **1**·toluene under vacuum results in loss of lattice toluene, as shown by elemental analysis and ^1H NMR spectroscopic studies. Yield: 0.04 g (10% based on Sn supplied). IR (Nujol, NaCl): ν/cm^{-1} ca. 3060(w) (C–H str.), other bands at 1095 (s), 1019 (s), 800 (s) (air-exposure leads to a broad O–H str. band centered at ca. 3350 cm^{-1} and to a P–H str. band at 2360 cm^{-1}). ^1H NMR (400.13 MHz, $\text{D}_8\text{-THF}$, $+25^\circ\text{C}$): δ ca. 8.7–6.6 (overlapping mult., Ph-H), 2.35 (mult., $-\text{CH}_2-$ PMDETA), 2.17 (s, Me-N PMDETA), 2.13 (s, Me_2N PMDETA). Anal. Found: C 50.3, H 6.8, N 9.9, P 10.5. Calcd for **1**: C 51.8, H 7.4, N 10.1, P 11.1.

Synthesis of 2. To a solution of pyPH_2 (0.42 mL, 5.0 mmol) in THF (20 mL) at -78°C was added $^n\text{BuLi}$ (3.1 mL, 1.6 mol L^{-1} , 5.0 mmol), giving an orange solution. The solution was warmed to room temperature and stirred for 4 h. The solution was then cooled to -78°C , and $\text{Sn}(\text{NMe}_2)_2$ (0.52 g, 2.5 mmol) in THF (10 mL) was added; the solution turned dark red immediately. The reaction mixture was allowed to stir at room temperature for 16 h. The solvent was removed, and **2**·2.5THF

(12) These interactions are typical of pyN donor interactions with $\text{Sn}(\text{II})$ and $\text{Sn}(\text{IV})$ (ca. 2.40–2.60 Å), for example: Jastrzebski, J. T. B. H.; Boersma, J.; Esch, P. M.; van Koten, G. *Organometallics* **1991**, *10*, 930.

(13) Hou, Z.; Stephan, D. W. *J. Am. Chem. Soc.* **1992**, *114*, 10088. Hou, Z.; Breen, T. L.; Stephan, D. W. *Organometallics* **1993**, *12*, 3158.

(14) Olmstead, M. M.; Power, P. P. *Inorg. Chem.* **1984**, *23*, 413.

(15) Spiegel, G. U.; Stelzer, O. *Chem. Ber.* **1990**, *123*, 989. Bulot, J. J.; Aboujaoude, E. E.; Colligon, N. *Phosphorus, Sulfur, Silicon* **1984**, *21*, 197.

(16) Hoffmann, D.; Bauer, W.; Hampel, F.; van Elkema Hommes, N. J. K.; Schleyer, P. v. R.; Otto, P.; Pieper, U.; Stalke, D.; Wright, D. S.; Snaith, R. *J. Am. Chem. Soc.* **1994**, *116*, 528.

was obtained as red crystals by storage at $-15\text{ }^{\circ}\text{C}$ from a THF/toluene (7:3 mL) solution. Placing crystals of **2**·2.5THF under vacuum prior to isolation results in loss of ca. 1.5 THF from the lattice, as shown by elemental analysis. Yield: 0.28 g (64% based on Sn supplied). ^1H NMR (400.13 MHz, $\text{D}_8\text{-THF}$, $+25\text{ }^{\circ}\text{C}$): δ ca. 8.2–6.7 (overlapping multiplets, 2-py), 3.60 (mult., THF), 1.78 (mult. THF). Anal. Found: C 33.3, H 3.8, N 8.9. Calcd for **2**·1THF: C 33.6, H 2.5, N 7.2.

Crystallographic Studies of 1 and 2. Crystals of **1** and **2** were mounted directly from solution under argon using an inert oil, which protects them from atmospheric oxygen and moisture. X-ray intensity data were collected using a Nonius Kappa CCD diffractometer. Details of the data collections and structural refinements are given in Table 1. The structures were solved by direct methods and refined by full-matrix least squares on F^2 .¹⁷ All hydrogen atoms in **1** and **2** are included in idealized positions. In **1** relatively high thermal parameters indicated considerable conformational disorder of the carbon atoms of the PMDETA coordinated to Na(2). Attempts to resolve the disorder were unsuccessful. Within the lattice there is half a molecule of toluene per asymmetric unit. Compound **2** contains a total of 2.5 molecules of lattice-bound THF solvent. One of these molecules is of full occupancy, and in addition

there are three sites, each of half-occupancy, corresponding to disordered solvent molecules in the vicinity of the inversion center. Atomic coordinates, bond lengths and angles, and thermal parameters for **1** and **2** have been deposited with the Cambridge Crystallographic Data Centre.

Acknowledgment. We gratefully acknowledge the EPSRC (M.McP., C.M.P., M.L.S., D.S.W.), The Cambridge European Trust (F.G.), The Newton Trust (F.G.), The States of Guernsey and The Domestic and Millennium Fund (R.A.K.), St. Catharine's College Cambridge (Fellowship for A.D.W.), and Churchill and Fitzwilliam Colleges Cambridge (A.D.H.) for financial support. Acknowledgment is made to the donors of the American Chemical Society Petroleum Research Fund for partial support of this research (M.L.S.). We also thank Dr. J. Davies for collecting X-ray data on **1** and **2**.

Supporting Information Available: Crystallographic data in CIF format for the structures and ^1H and $^{31}\text{P}\{^1\text{H}\}$ NMR spectra of **1** and **2**. This material is available free of charge via the Internet at <http://pubs.acs.org>.

(17) Sheldrick, G. M. *SHELX-97*; Göttingen, Germany, 1997.